



## Analysis of Mosha fault by using earthquake focal mechanism

A. Gholamzadeh<sup>1</sup> Sh. Pourbeyranvand<sup>2</sup>, M. Reguzzoni<sup>3</sup>, L. Rossi<sup>4</sup>,

<sup>1</sup>, Politecnico di Milano, [amirhossein.gholamzadeh@mail.polimi.it](mailto:amirhossein.gholamzadeh@mail.polimi.it)

<sup>2</sup>Assistant Professor, Seismology Dept., International Institute of earthquake engineering and seismology.  
[beyranvand@iiees.ac.ir](mailto:beyranvand@iiees.ac.ir)

<sup>3</sup>DICA, Politecnico di Milano, Piazza Leonardo da Vinci 32, 20133 Milano, Italy [mirko.reguzzoni@polimi.it](mailto:mirko.reguzzoni@polimi.it)

<sup>4</sup>PhD program in environmental and infrastructural engineering  
[lorenzo.l.rossi@polimi.it](mailto:lorenzo.l.rossi@polimi.it)

### Abstract:

We used the focal mechanism of crustal earthquakes to estimate the magnitude and direction of the maximum principal stress near Tehran. Our assumptions are that the slip vector lies in the fault plane and is parallel to the maximum resolved shear stress in that plane. The theoretical analysis is tested using accurately determined focal mechanisms of 51 earthquakes) that occurred along the Mosha fault. The earthquake focal mechanisms in the Central Alborz are divided into seven groups with respect to their location. The method that applied here is based on a developed stress inversion of Michael proposed by Vaclav Vavrycukin 2014 by applying the fault instability constraint and the stress is calculated by iterations.

**Keywords:** Focal mechanism, Stress inversion, Maximum principal stress, Mosha fault.

\*Author: Amirhossein Gholamzadeh

### Introduction

The study area in the southern slopes of the Central Alborz Mountain range between latitudes 34 to 36° north and length 51 to 54° east and part of the edge South of Central Alborz. The Mosha fault is located east of Tehran, the densely populated capital city of Iran. Due to some reasons study of this fault is of great importance, firstly, the activity of this fault, secondly, large historical earthquakes that occurred and finally its closeness to the city of Tehran.

By this analysis, we can see that the direction of the maximum compression stress field has a strong impact on the propensity of the rupture path to bend on to the potential branch path and to control the arrest or further propagation of rupture. Our aim, in this paper, is to use all available geodetic data and focal mechanism of earthquakes to determine a stress map of Mosha fault. If we assume that stresses in a continuum are produced by the application of tectonic forces and its consequent deformation on the crustal scale, then the direction of the principal components of the stress and strain (or strain rate) tensors must ideally be the same. In the next sections we present the analysis of the various seismic and geodetic data. We combine these multidisciplinary data to produce the stress map. This stress map is then used to discuss the various tectonic regimes in Mosha fault.

Finally based on maximum horizontal stress, we use these data to analyze them in the same map of the Central Alborz area. The focal mechanism data are collected from published papers using local seismic networks (Tatar et al. 2012), and CMT solutions from the Global Centroid Moment Tensor Project (GCMT). The local focal mechanisms were derived based on polarity readings of the first P-wave motion of local earthquakes (Snook et al. 1984).



## Methodology

### Focal mechanisms Stress Inversion (Michael, 1984)

A widely used method for deriving stress field at seismic depths is inversion of earthquake focal mechanisms [e.g., Michael, 1984, 1987; Heidbach, 2010]. This method is based on two assumptions: first, that the tangential traction on the fault plane should be parallel to the slip direction and, second, that the stress field is uniform for the data set.

If the above-mentioned assumptions are satisfied, the stress inversion methods can determine four parameters of the stress tensor: three angles defining the directions of principal stresses,  $\sigma_1$ ,  $\sigma_2$  and  $\sigma_3$ , and shape ratio  $R$  (Gephart & Forsyth 1984):

$$R = \frac{\sigma_1 - \sigma_2}{\sigma_1 - \sigma_3} \quad (1)$$

The tangential traction on the plane tends to be parallel to the slip direction:

$$\hat{\tau} = \frac{\bar{\tau}(\hat{n}, \sigma)}{|\bar{\tau}(\hat{n}, \sigma)|} = \hat{s} \quad (2)$$

in which  $\bar{\tau}(\hat{n}, \sigma)$  is the tangential traction on the fault plane with a unit normal  $\hat{n}$  due to the deviatoric stress tensor  $\sigma$ . When we assume that the stress field is constant within the region of the study during the faulting event, means that by solving (1), for several faults, a single  $\sigma$  that best satisfies all the fault is found. Also, we can solve (2) linearly, by considering that  $|\bar{\tau}| = 1$ . (Michael, 1984).

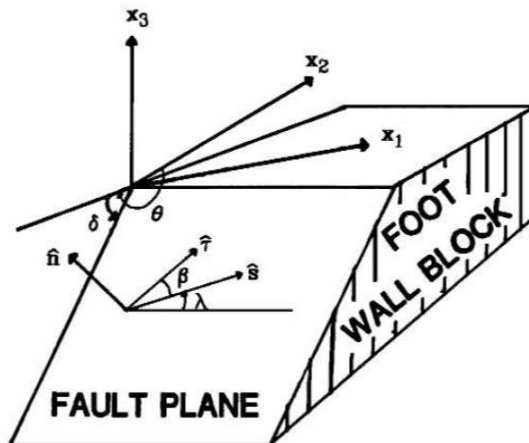


Fig 1. The  $\theta$ ,  $\delta$  and  $\lambda$  are dip direction, the dip, and the rake, respectively.  $\hat{n}$  and  $\hat{s}$  are the outward normal to the foot wall block and slip vector, respectively (Michael 1987).



## Stress inversion

### Focal mechanisms Stress Inversion (Vavryčuk, 2014)

the inversion would provide high-resolution information on natural variations of the stress field. The ambiguity of identifying the fault plane in focal mechanisms introduces difficulties also in other stress inversion methods. One way of identifying the fault plane is evaluating the fault instability  $I$  proposed by Vavryčuk et al. (2013):

$$I = \frac{\tau - \mu(\sigma - \sigma_1)}{\tau_c - \mu(\sigma_c - \sigma_1)} \quad (1)$$

where  $\tau_c$  and  $\sigma_c$  are the shear traction and effective normal traction along the optimally oriented fault (Fig. 2, red dot), and  $\tau$  and  $\sigma$  are the shear traction and effective normal traction along the analyzed fault plane (Fig. 2, black dot) (Vavryčuk, 2014).

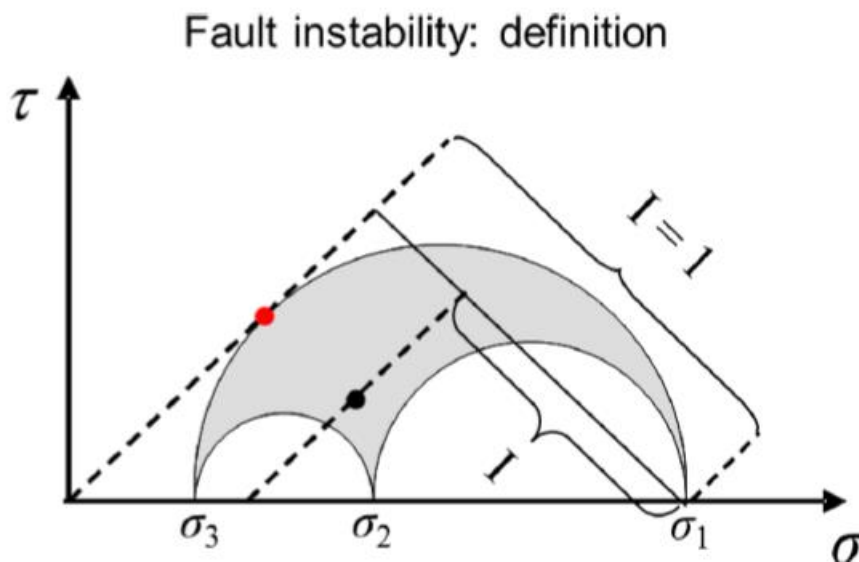


Fig 2. Definition of the fault instability in Mohr's diagram. The red dot marks the tractions on the principal fault characterized by instability  $I = 1$ . The black dot marks the tractions of an arbitrarily oriented fault with instability  $I$ . (Vavryčuk, 2014).

## Application

### STRESSINVERSE

To analyze the data, for stress inversion, we use a MATLAB code, "STRESSINVERSE" Version 1.1.3, .2020, Author: Václav Vavryčuk.

STRESSINVERSE is a MATLAB software package for an iterative joint inversion for stress and fault orientations from focal mechanisms. The inversion is based on Michael's method (1984, 1987) in which an instability criterion proposed by Lund & Slunga (1999) is incorporated.

### Win Tensor

In this study we also use another way to compute stress field by using TENSOR program.

Therefore, we used two different stress inversion methods: the Right Dihedron and Rotational Optimization methods of Delvaux and Sperner (2003).



### Improved Right Dihedron method

According to Abdalnaby et al. (2014), the Right Dihedron method was originally a graphical Method developed by Angelier and Mechler (1977) to determine the range of possible  $\sigma_1$  and  $\sigma_3$  stress axes orientations in fault analysis. This method has two limitations. First, it does not determine the stress ratio. Second, it does not define  $\sigma_1$  and  $\sigma_3$  when the extreme values on the counting net do not reach 0 and 100%. Delvaux and Sperner (2003) developed this method by removing these two limitations and enabled the Improved Right Dihedron method to determine the stress ratio and define  $\sigma_1$  and  $\sigma_3$  even under extreme cases (see Delvaux and Sperner, 2003 for details). The results of this method are used as a starting point for the Rotational Optimization Method.

### Rotational Optimization method

This method is a new iterative inversion procedure presented by Delvaux and Sperner (2003). It aims to minimize a misfit function through a grid search of many different stress tensors. In this method, both nodal planes of each focal mechanism are compared to a stress tensor, and the plane that has the smaller value of the misfit will be considered as the actual fault plane. This means that we do not need to specify which nodal plane is the fault plane prior to the inversion routine. After this separation the final inversion includes only the focal planes that are best fitted by a uniform stress field. The selected fault planes are then inverted to calculate the principal stress axes and the stress ratio (Gephart and Forsyth, 1984). The results are plotted on an equal-area projection to allow us to evaluate the overall quality of the result. Formal stress inversion of the focal mechanisms data is based on two assumptions (Mercier et al., 1991; Carey-Gailhardis and Vergely, 1992): (a) the stress field is uniform and invariant in space and time, and (b) earthquake slip occurs in the direction of maximum shear stress (Wallace Bott hypothesis, Bott, 1959). The angle between the calculated shear stress and the slip vector  $d$  is the fit angle  $\alpha$ . Thus, the corresponding misfit function to be minimized for each earthquake is the misfit angle  $\alpha$  (Delvaux and Sperner, 2003). We process the data interactively, first using the "Right Dihedron Method", a graphical method for determination of the range of possible orientations  $\sigma_1$  and  $\sigma_3$ , which is independent from the choice of the nodal planes (Angelier, 1994; Angelier and Mechler, 1977). This method allows a first estimation of the orientations of the principal stress axes and of the stress ratio  $R$ , and a first filtering of compatible fault-slip data (Delvaux and Barth, 2010). The selected fault-slip data and the preliminary tensor can be used as a starting point in the iterative grid search inversion procedures of the Rotational Optimization method. It allows restriction of the search area during the inversion, so that the whole grid does not have to be searched (Delvaux and Barth, 2010). It minimizes the misfit angle  $\alpha$  using the stress tensor that is being tested, but also favors higher shear stress magnitudes and lower normal stress magnitudes on the plane to promote slip (Delvaux and Barth, 2010). To numerically express the stress regime, we use the stress regime index  $R'$ , based the value of the stress ratio ( $R$ , Eq. (1)) and the type of stress regime as described in Delvaux et al. (1997, 2007) and Delvaux and Sperner (2003). The tectonic stress regime index  $R'$  is defined as:

$R' = R$  for normal faulting regimes (NF).

$R' = (2 - R)$  for strike-slip regimes (NS); and

$R' = (2 + R)$  for thrust faulting regimes (TF).

### Zonation and area definition

Since the focal mechanism data over the entire study area are not consistent in terms of stress regime and stress orientation, it cannot all be inverted altogether. Therefore, we divide the region into seven clusters areas based on their geographical proximity, kinematic homogeneity, tectonic setting, and the greatest density of similar focal mechanisms, to study the regional changes in stress orientation.



## Input data

The data that we have used are coming from, 10 focal mechanisms from GCMT + 51 focal mechanisms from Tatar et al. (2012).

Table 1. earthquake focal mechanism parameters, divided into seven clusters.

Clusters	Num	Long (°E)	Lat (°N)	Depth (km)	Focal plane			Quality
					Strike	Dip	Rake	
A1	1	51.78	35.72	11.6	95	15	70	B
	2	51.79	35.7	4.8	80	55	-119	B
	3	51.8	35.7	2	105	45	-71	A
	4	51.76	35.68	7.2	80	60	-151	B
	5	51.86	35.64	15	80	70	27	B
	6	51.86	35.59	11.2	340	60	-79	A
A2	1	51.83	35.82	3.9	275	50	7	B
	2	51.87	35.81	8.6	85	45	20	A
	3	51.88	35.79	9.6	280	55	64	A
	4	51.9	35.79	12.6	160	85	134	B
	5	51.87	35.73	5.4	310	60	-70	B
	6	51.89	35.73	4.6	140	40	-47	A
A3	1	52	35.61	12.7	320	70	-141	B
	2	52.01	35.62	6.8	20	85	-45	B
	3	52.05	35.58	10.4	75	80	26	A
	4	52.07	35.63	15	130	50	36	B
	5	52.07	35.66	18.5	55	60	-49	B
A4	1	52.33	35.64	5.9	310	80	0	B
	2	52.39	35.64	2	110	50	-76	B
	3	52.36	35.7	9.9	260	70	-14	A
	4	52.38	35.7	13.5	265	70	-14	B
	5	52.41	35.69	5.9	75	75	18	B
	6	52.46	35.71		348	32	-41	C
	7	52.58	35.62	7.7	195	70	-14	B
	8	52.66	35.62	9.3	30	55	-39	B
A5	1	52.34	35.87	8.1	70	65	-22	B
	2	52.24	35.76	11.3	205	60	-170	B
	3	52.27	35.78	10.7	130	80	-80	B
	4	52.34	35.77	14.4	85	40	90	B
	5	52.36	35.77	7.1	270	55	84	B
A6	1	52.11	35.77	12	270	50	179	A
	2	52.1	35.74	11.7	40	89	179	A
	3	52.1	35.75		255	70	-14	A
	4	52.08	35.73	7.4	225	70	179	B
	5	52.15	35.74	4.4	265	80	26	A
	6	52.14	35.72	4.4	265	85	45	A
A7	1	51.98	35.78	10.2	190	80	0	A
	2	52	35.77	17.4	170	80	45	B
	3	52.01	35.78		210	60	-170	A
	4	52.01	35.79	15	95	70	179	A
	5	52.02	35.73	10	300	45	-49	A
	6	52.03	35.77	11.3	270	70	179	A
	7	52.04	35.74	15	325	30	58	B





## Results

I have performed a formal stress inversion by these two methods (Delvaux and Sperner, 2003 and Vavrycuk, 2014), for the first cluster and the same procedure has been applied to all remaining clusters, so, you can see the summary of the results in Table 2 and Fig.4. The results show that there are differences of the value of SHmax between two methods because in the analysis with win tensor, the software for defining the fault plane will eliminate invalid data to minimize the misfit function. Anyway, we can see that there is a good agreement between both methods to identifying the orientation of the principal axes.

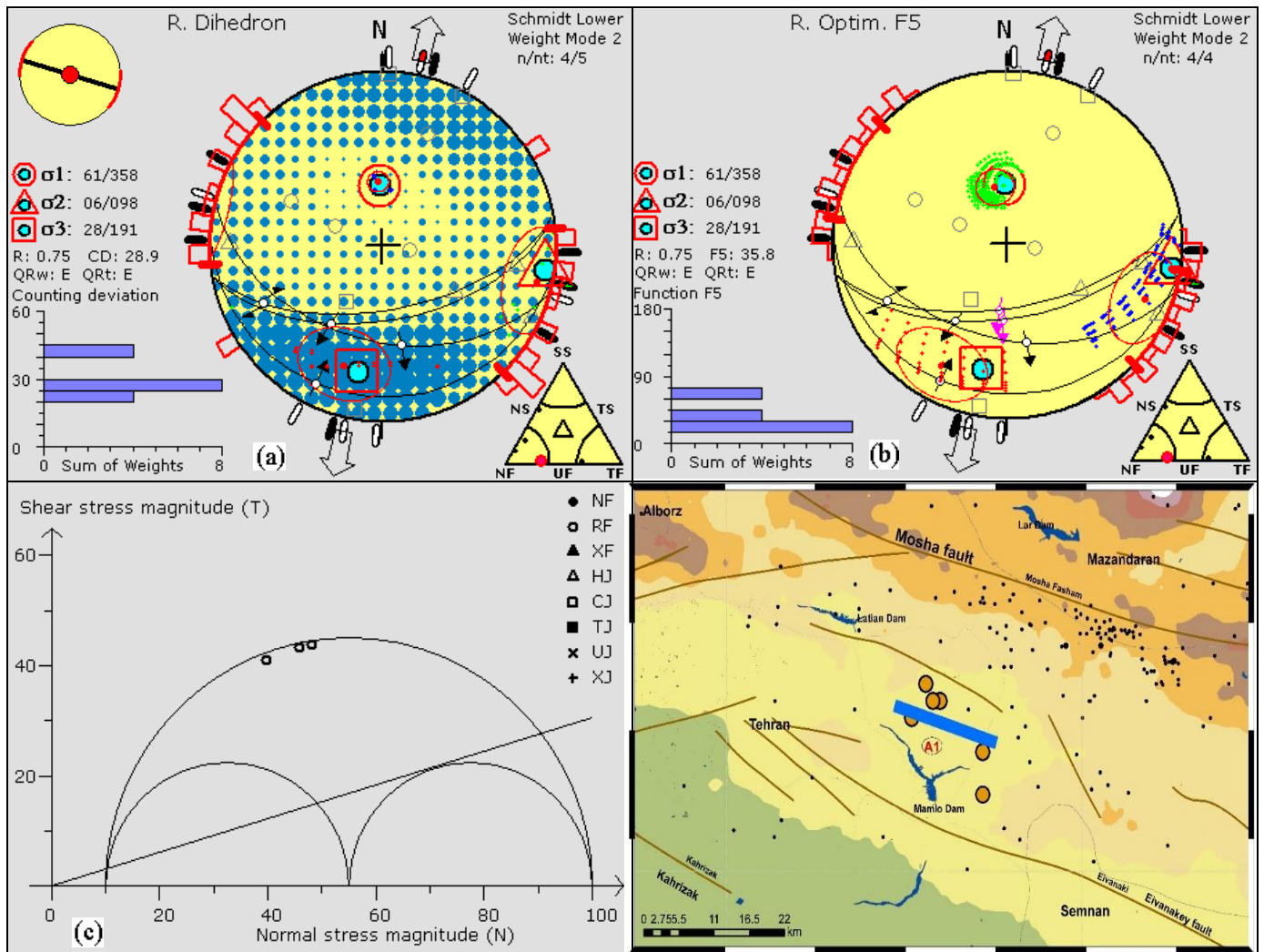


Figure 3(a). Formal stress inversion of the focal mechanisms data based on Table 1 (Win Tensor)

tensor solutions in the study area: a) Right Dihedron method, green arrows for maximum principal compression, red arrows for minimum principal compression, the histogram gives the counting deviation angles. b) Rotational Optimization, blue arrows for maximum principal compression, red arrows for minimum principal compression, the histogram gives the distribution of measured data against the function F5. For best fit F5 approaches 0 for all measurements. c) Mohr diagram illustrates the stress regime, and the area of fault activation is constrained by the three circles and the line of initial friction corresponding to an angle of 16.7°.



Cluster A1 is located between 51.76°- 51.86° E and 35.58°- 35.72° N and it contains six focal mechanisms for this sub-area. Focal mechanisms are dominantly Normal faulting. The resulting stress tensor suggests that the stress field is homogeneous in a NE-SW orientation ( $N18 \pm 5^\circ E$ ), and the stress ratio  $R = 0.75$ . and the stress regime  $R' = R$  for Normal faulting. Moreover, the direction of  $SH_{max} = N107^\circ E$ .

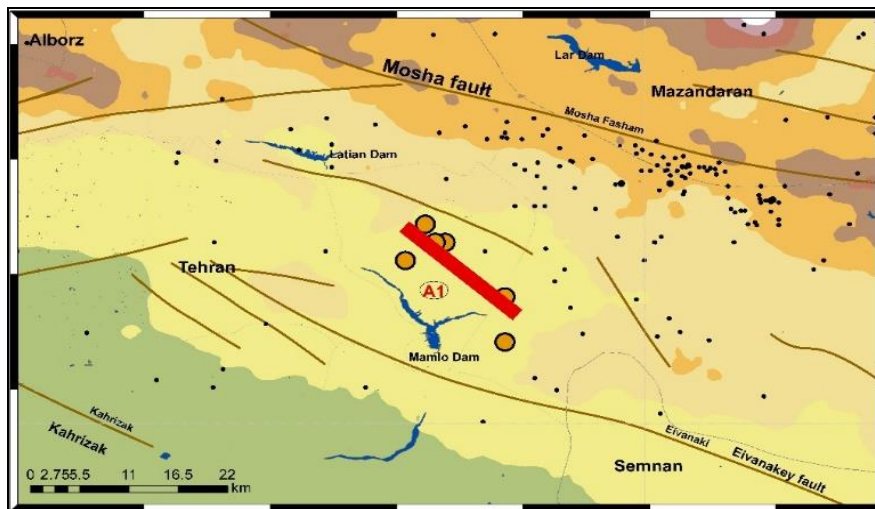
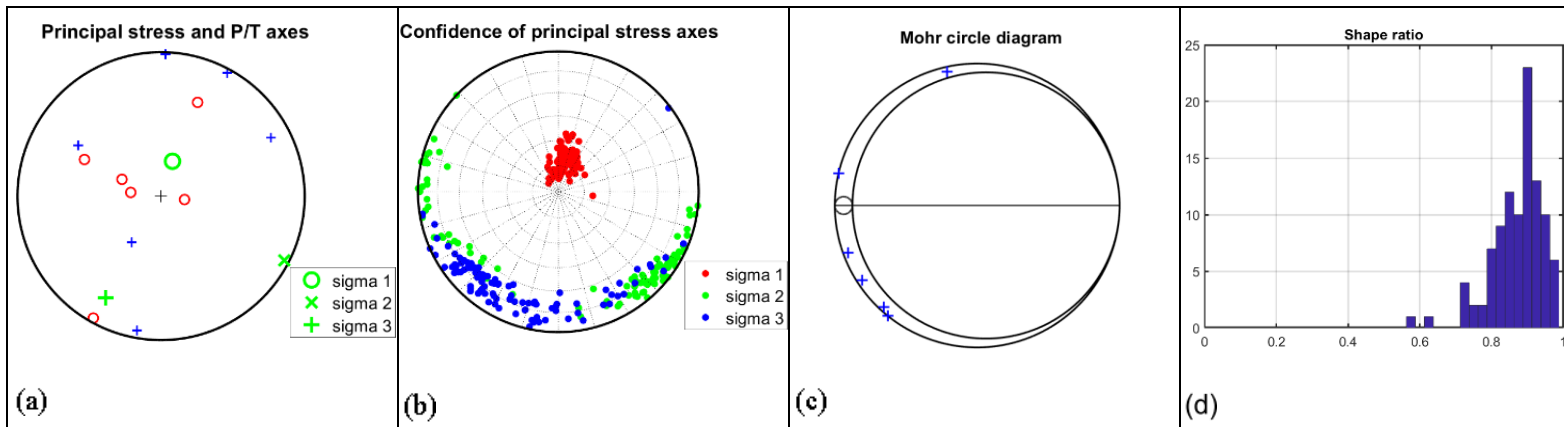


Figure 3(b). Formal stress inversion of the focal mechanisms data based on Table 1 (Stressinverse)

- (a) P/T axes with retrieved principal stress directions, (b) the P/T axes, (c) Mohr's circle diagram with positions of faults (blue plus signs), (d) define the distributions of the shape ratio calculated using the iterative method.

The same as Fig 3(a), the differences are for the value of  $R = 0.9$  and the direction of  $SH_{max} = N130.68^\circ E$ . The direction of the maximum horizontal stress is from NW-SE (same as Win Tensor).

The difference between the methods may be because Win Tensor eliminates incompatible data. By the way, this difference is not so high. The orientation of the principal axes of both methods is similar.



Table 2. (a) Win tensor

Area	Stress tensor parameters			Shmax(°)	Stress regime
	$\sigma_1$	$\sigma_2$	$\sigma_3$		
A1	61/358	06/098	28/191	107	Normal-Fault
A2	06/219	41/315	48/122	37	thrust faulting
A3	32/193	57/030	08/288	16	Strike-Slip
A4	07/215	82/062	04/305	37	Strike-Slip
A5	53/044	26/275	25/172	54	Normal-Fault
A6	00/065	62/335	28/155	65	Strike-Slip
A7	00/308	73/217	17/038	128	Strike-Slip

Table 2. (b) Stressinverse

Area	Stress tensor parameters			Shmax(°)	Stress regime
	$\sigma_1$	$\sigma_2$	$\sigma_3$		
A1	69/18	04/117	20/209	131	Normal-Fault
A2	39/206	41/71	25/318	29	Unclassified
A3	80/33	85/27	01/285	15	Normal-Fault
A4	80/33	10/206	01/296	27	Normal-Fault
A5	30/33	01/302	60/210	34	Thrust -fault
A6	31/58	43/294	31/169	60	Unclassified
A7	0.9/287	83/24	07/197	107	Strike-Slip

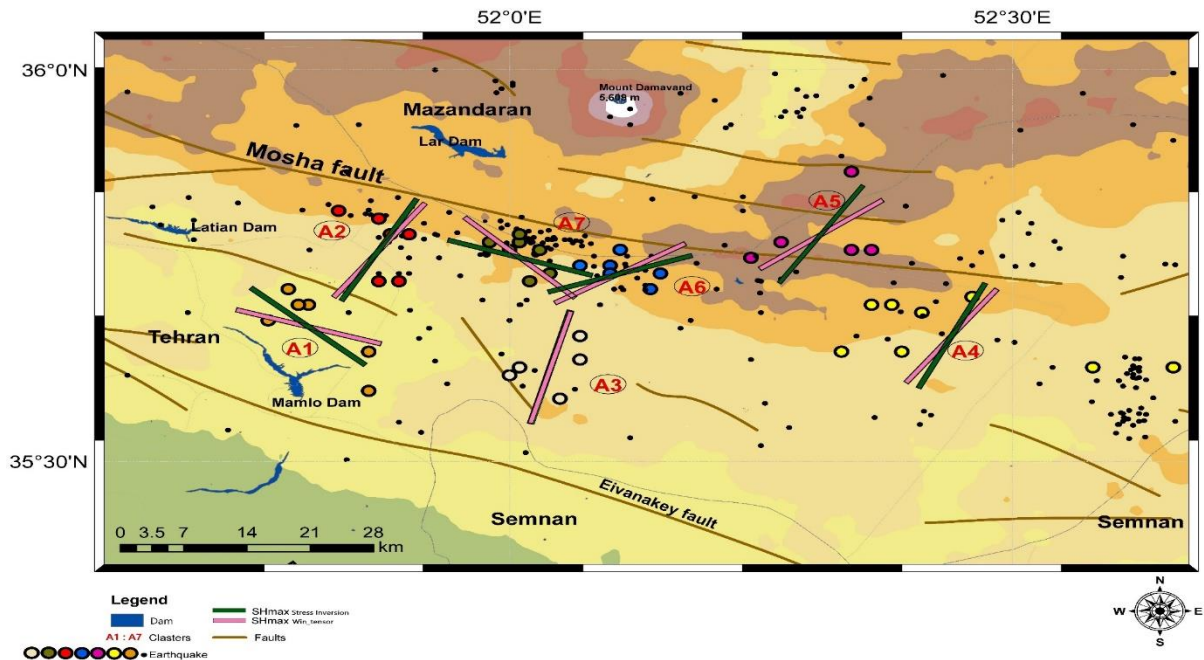


Fig 4. Comparison of SHmax obtained from Stressinverse and win tensor software, green and pink bar, respectively.

## Discussion

In this study our approach was to estimate the direction of the stress from earthquake focal mechanism, our network including seven clusters was installed to investigate the faults surrounding the city of Tehran. The Central and Eastern segments of the Moshafault, area A3, A4, A6 and A7 are





strike-slip mechanism, with compound nature of faulting, some normal events also occur at A1 and A5 due to the local tectonic environment. The direction of the stress for all clusters represents SW-NE except for A1 and A7 that are NW-SE, for these two clusters also we have maximum difference between Win tensor result and stress inversion result. Moreover, we are witnessing a high density of earthquake in the area A3, A6 and A7 that have strike-slip mechanism, The directions of the maximum horizontal stresses in the study area agree with the existing geological facts. As we go far from the location of the fault the number of earthquakes decreasing so we can say that there is a direct link between the presence of the active fault and occurring of earthquake (Bahirae 2013). Extraordinary socio-economic importance of the country capital and from one side the environment and the existence of active seismic structure and imminent threatening on the other hand, emphasis on necessity of designing and operating the monitoring and warning system Instant Earthquake Danger (Earthquake Idea can be done also by installing the right number of Monitoring and Early Warning System). This seismic stations and equipment, intelligent control, and earthquake Risk Management tools (Seismic Risk Management).

## Conclusions

We show that the focal mechanism of the 51-earthquake divided into the 7 clusters for area of the Mosha fault that located between  $34^{\circ}$ -  $36.5^{\circ}$  N and  $51^{\circ}$ -  $53.5^{\circ}$  E. This tells us that most of our mechanisms are Strike-slip along the Mosha fault. Our study investigates the faults surrounding the city of Tehran: The Central and Eastern segments of the Mosha fault. The method which is applied here for the stress inversion proposed by Michael (1984) with a linear algorithm and due to uncertainties associated with stress field a nonlinear method (Vavrycuk 2014) is used which is done by MATLAB code, also we perform a formal inversion to determine the present-day stress field. We used two different stress inversion methods: Right Dihedron and the Rotational Optimization methods of Delvaux and Sperner (2003). It can help to define the geometry and motion of the associated fault. As mentioned, the aim of this study is to find the direction of the main stresses and the maximum horizontal stress by using inversion of focal mechanisms proposed by Vavrycuk inversion method. The horizontal stress orientations are usually expressed in terms of SHmax (maximum horizontal stress axis) and SHmin (minimum horizontal stress axis), which are perpendicular to each other. There are two methods to calculate the horizontal stress axes (for more details see Zoback, 1992a and Lund and Townend, 2007). The Lund and Townend method are applied in the Win-tensor program, and it is used in this study. Detailed results are obtained using Win Tensor to analyze the 51 available focal mechanisms (Fig. 3).

## References

- Angelier, L., 1994. Faults slip analysis and paleostress reconstruction. In: Hancock, P.L. (Ed.), Continental Deformation. Pergamon, Oxford, pp. 101e120
- Bott, M.H.P., 1959. The mechanisms of oblique slip faulting. *Geol. Mag.* 96, 109e117.
- Delvaux, D., Moeys, R., Stapel, G., Petit, C., Levi, K., Miroshnichenko, A., Ruzhich, V., Sankov, V., 1997. Paleostress reconstructions and geodynamics of the Baikal region, Central Asia. Part II: Cenozoic rifting. In: Cloetingh, S., Fernandez, M., Munoz, J.A., Sassi, W., Horvath, F. (Eds.), Structural Controls on Sedimentary Basin Formation: Tectonophysics, 282, pp. 1e38.
- Gephart, J. W. and Forsyth, D. W., 1984- An Improved Method for Determining the Regional Stress Tensor Using Earthquake Focal Mechanism Data: Application to the San Fernando Earthquake Sequence, *J. Geophys. Res.*, 89, 9305-9320.
- Khorrami, F., Hesami, Kh., Nankali, H.R., Tavakoli, F., 2012. *Geosciences. Geol Surv Iran* 82:223–230
- Lund, B. and Slunga, R., 1999- Stress tensor inversion using detailed microearthquake information and stability constraints: Application to Olfus in southwest Iceland, *Journal of Geophysical Research*, 104(B7), 14947-14964.
- Lund, B., Townend, J., 2007. Calculating horizontal stress orientations with full or partial Knowledge of the tectonic stress tensor. *Geophys. J. Int.* 270, 1328e1335.



- Masson, F., Chery, J., Hatzfeld, D., Martinod, J., Vernant, P., Tavakoli, F. and Ghafory-Ashtiani, M., 2005- Seismic versus aseismic deformation in Iran inferred from earthquakes and geodetic data, *Geophys. J. Int.*, 160, 217–226
- Michael, J., 1984- Determination of Stress from Slip Data: Faults And Folds, *Journal of Geophysical Research*, VOL. 89, No. B13, Pages 11,517-11,526
- Nilfouroushan, F., Masson, F., Vernant, P., Vigny, C., Martinod, J., Abbassi, M., Nankali, H., Hatzfeld, D., Bayer, R., Tavakoli, F., Ashtiani, A., Doerflinger, E., Daignières, M., Collard, P. and Chéry, J., 2003- GPS network monitors the Arabia-Eurasia collision deformation in Iran, *Journal of Geodesy*, 77, 411-422.
- Pourbeyranvand, sh., 2018. Stress studies in the Central Alborz by inversion of earthquake focal mechanism data.
- Raeesi, M., Zarif, Z., Nilfouroushan, F., Boroujeni, S.A., Tiampo, K., 2016. Quantitative analysis of seismicity in Iran. *Pure Appl Geophys* 174(3):793–833. <https://doi.org/10.1007/s00024-016-1435-4>
- S. Bahirae, M. Arian, M. Ghorashi and A. Solgi. The movement potential evolution of the Mosha fault. 2013 January 13.
- Tatar, M., Hatzfeld, D., Abbassi, A. and Yamini Fard, F., 2012- Microseismicity and seismotectonics around the Mosha fault (Central Alborz, Iran), *Tectonophysics*, Volumes 544–545, 29 May 2012, Pages 50–59.
- Vavryčuk V (2014) Iterative joint inversion for stress and fault orientations from focal mechanisms. *Geophys J Int* 199(1):69–77. <https://doi.org/10.1093/gji/ggu224>
- Vavryčuk, V., Bouchaala, F. & Fischer, T., 2013. High-resolution fault image from accurate locations and focal mechanisms of the 2008 swarm earthquakes in West Bohemia, Czech Republic, *Tectonophysics*, 590, 189–195.
- Zarifi, Z., Nilfouroushan, F. and Raeesi, M., 2014- Crustal stress map of Iran: Insight from seismic and geodetic computations. *Pure and Applied Geophysics*, 171, 1219–1236
- Zarifi, Z., Nilfouroushan, F. and Raeesi, M., 2014- Crustal stress map of Iran: Insight from seismic and geodetic computations. *Pure and Applied Geophysics*, 171, 1219–1236.